

On the nature of the Møller-Plesset critical point

Cite as: J. Chem. Phys. **123**, 064105 (2005); <https://doi.org/10.1063/1.1991854>

Submitted: 02 July 2004 . Accepted: 09 June 2005 . Published Online: 16 August 2005

Alexey V. Sergeev, David Z. Goodson, Steven E. Wheeler, and Wesley D. Allen



View Online



Export Citation

ARTICLES YOU MAY BE INTERESTED IN

[Is Møller-Plesset perturbation theory a convergent ab initio method?](#)

The Journal of Chemical Physics **112**, 9213 (2000); <https://doi.org/10.1063/1.481764>

[Gaussian basis sets for use in correlated molecular calculations. I. The atoms boron through neon and hydrogen](#)

The Journal of Chemical Physics **90**, 1007 (1989); <https://doi.org/10.1063/1.456153>

[Why does MP2 work?](#)

The Journal of Chemical Physics **145**, 184101 (2016); <https://doi.org/10.1063/1.4966689>

The Journal
of Chemical Physics

2018 EDITORS' CHOICE

READ NOW!



On the nature of the Møller-Plesset critical point

Alexey V. Sergeev and David Z. Goodson^{a)}

Department of Chemistry and Biochemistry, University of Massachusetts Dartmouth, North Dartmouth, Massachusetts 02747-2300

Steven E. Wheeler and Wesley D. Allen^{b)}

Center for Computational Chemistry, University of Georgia, Athens, Georgia 30602-2525

(Received 2 July 2004; accepted 9 June 2005; published online 16 August 2005)

It has been suggested [F. H. Stillinger, *J. Chem. Phys.* **112**, 9711 (2000)] that the convergence or divergence of Møller-Plesset perturbation theory is determined by a critical point at a negative value of the perturbation parameter z at which an electron cluster dissociates from the nuclei. This conjecture is examined using configuration-interaction computations as a function of z and using a quadratic approximant analysis of the high-order perturbation series. Results are presented for the He, Ne, and Ar atoms and the hydrogen fluoride molecule. The original theoretical analysis used the true Hamiltonian without the approximation of a finite basis set. In practice, the singularity structure depends strongly on the choice of basis set. Standard basis sets cannot model dissociation to an electron cluster, but if the basis includes diffuse functions then it can model another critical point corresponding to complete dissociation of all the valence electrons. This point is farther from the origin of the z plane than is the critical point for the electron cluster, but it is still close enough to cause divergence of the perturbation series. For the hydrogen fluoride molecule a critical point is present even without diffuse functions. The basis functions centered on the H atom are far enough from the F atom to model the escape of electrons away from the fluorine end of the molecule. For the Ar atom a critical point for a one-electron ionization, which was not previously predicted, seems to be present at a positive value of the perturbation parameter. Implications of the existence of critical points for quantum-chemical applications are discussed. © 2005 American Institute of Physics. [DOI: 10.1063/1.1991854]

I. INTRODUCTION

Although Møller-Plesset (MP) perturbation series are not typically computed beyond fourth order in practical applications, it is possible to use full-configuration-interaction (FCI) methodology to obtain the series coefficients up to much higher orders^{1,2} in order to study the series convergence. FCI computations are very demanding but are now feasible using reasonably large basis sets for systems with as many as eight or so correlated electrons, and consequently a fair number of high-order MP series are now available in the literature.³⁻⁵ Perhaps the most surprising result of these studies is the discovery that many of the series are divergent.

Among the divergent cases are such systems as Ne, F⁻, HF, Cl⁻, and OH⁻. These have “class B” series, so called because their series coefficients, once beyond the lowest orders, alternate in sign.⁶ Cremer and co-workers^{7,8} have argued that the sign alternation results from the concentration of electron pairs in small regions of space, as in closed-shell systems with highly electronegative elements. It is interesting that the divergence can depend strongly on the nature of the basis set. A vivid illustration was given by Olsen *et al.*,⁴ who showed that the F⁻ series, which is strongly divergent with the augmented correlation-consistent polarized valence double-zeta (aug-cc-pVDZ) basis set, becomes convergent

when the diffuse functions are replaced with an equal number of compact functions from the succeeding triple-zeta basis.

A useful approach to understanding the series divergence is to analyze the MP approximation for the energy as a continuous function of a perturbation parameter. MP perturbation theory can be formulated⁹ in terms of a partitioning of the Hamiltonian $H(z)$ according to

$$H(z) = H_0 + zH_1, \quad H_1 = H_{\text{phys}} - H_0, \quad (1)$$

where H_0 is the sum of one-electron Fock operators, H_{phys} is the actual Schrödinger Hamiltonian, and z is a continuous perturbation parameter. Then the MP perturbation series is the asymptotic series of the ground-state energy expanded about the point $z=0$. This series can be studied using methods of functional analysis in the complex plane.¹⁰ The series will diverge if a singular point exists in the disk of unit radius centered at the origin.¹¹ If this singularity lies on the negative real axis then the series coefficients will have alternating signs.¹²

An explanation for the existence of a singularity on the negative real axis has been presented by Stillinger.¹³ A negative value of the perturbation parameter corresponds to an unphysical situation in which the interelectron Coulomb potential is attractive. Stillinger argued that at a sufficiently negative value of the parameter, the system will dissociate into a bound electron cluster free from the nuclei. This value

^{a)}Electronic mail: dgoodson@umasds.edu

^{b)}Electronic mail: wdallen@ccqc.uga.edu

is a critical point at which the ground-state energy function has a branch-point singularity, at which the function remains finite but becomes multiple valued, with discontinuous derivatives. If the critical point comes before $z=-1$, the series diverges.

Here we examine Stillinger's conjecture for the noble-gas atoms He, Ne, and Ar and for the hydrogen fluoride molecule using configuration-interaction (CI) computations of the energy spectrum as a function of the perturbation parameter and analysis of high-order series with summation approximants. In particular, we consider the effect of the choice of basis set. This will clarify a statement by Forsberg *et al.*⁸ that the convergence of MP series can be improved by excluding diffuse functions from the basis set. For basis sets that contain diffuse functions, we find evidence of the existence of a critical point at negative z at the border of a dissociation continuum. However, this continuum corresponds to full ionization, with all electrons at infinite separation. The continuum corresponding to the electron cluster is not seen because standard basis sets are constructed from functions centered at the atomic nuclei and therefore cannot efficiently model an electron cluster dissociated from the nuclei. This cluster continuum does, however, appear if a specially designed nonstandard basis set is used.

Our analysis suggests that in certain cases a critical point can be present even with compact basis sets. Compact functions centered on an atom at one end of a molecule can provide enough basis flexibility to model the tunneling of electrons out of a potential-energy well at the other end when z is sufficiently negative. Also, a critical point at positive z , corresponding to one-electron ionization, can sometimes exist.

We begin with a review of the analysis of the Hamiltonian that implies the existence of a critical point. Then in Sec. III we explore the structure of the eigenvalue spectrum as a function of the perturbation parameter using CI computations. In Sec. IV we use summation approximants to determine singularity positions from high-order MP series, for comparison with the CI analysis. In Sec. V implications for quantum-chemical applications are discussed.

II. EXISTENCE OF A CRITICAL POINT

The perturbation expansion for the ground-state energy eigenvalue of the Hamiltonian H of Eq. (1) is obtained as a power series in z ,

$$E(z) = \sum_{i=0}^n E_i z^i. \quad (2)$$

The coefficient E_0 is equal to the sum of Hartree-Fock orbital energies, and $E_0 + E_1$ is the Hartree-Fock approximation for the total energy. At $z=1$ we have $H=H_{\text{phys}}$ and $E=\sum_{i=0}^n E_i$. If the perturbation series is convergent, then in the limit of large n this sum corresponds to the physical solution for the ground-state energy. The series will diverge if $E(z)$ contains a singular point within the disk of unit radius centered at the origin in the complex z plane.¹¹

Let us summarize and clarify the arguments of Stillinger¹³ for the existence of a singularity at negative z .

The r_{ij}^{-1} terms in H_{phys} , which represent the potential energy between electrons, are replaced in H_0 by a repulsive mean-field potential. The operator H_{phys} in Eq. (1) is multiplied by z . This means that when z is negative, the exact r_{ij}^{-1} interaction among electrons is mutually attractive while the mean-field interaction remains repulsive. The mean-field potential arises from a static negative charge cloud distributed according to the ground-state Hartree-Fock orbitals, which are localized about the nuclear framework. As the magnitude of z increases along the negative axis, the mean-field repulsive potential in H_0 becomes stronger because it is multiplied by a factor of $(1-z)$.

For sufficiently large negative z , a configuration in which the nuclei are infinitely separated from a bound cluster of electrons will have a lower energy than any completely bound state. The reason for this peculiar circumstance is two-fold.

- (1) The mean-field repulsion existing in the vicinity of the nuclei overwhelms the electron-nucleus attractions, thereby pushing the electrons toward infinity.
- (2) The r_{ij}^{-1} interelectron interactions, which are now attractive, persist outside the nuclear region.

The point z_c at which the energy of the bound ground state is equal to the energy of the electron cluster is expected to be a singular point of the function $E(z)$.

This analysis can be made more precise as follows. The electronic potential-energy operator in H is

$$V(z) = V^{(\text{ne})} + V^{(\text{ee})}(z), \quad (3)$$

in which $V^{(\text{ne})}$ is the Coulomb attraction between nuclei and electrons and $V^{(\text{ee})}$ is the z -dependent operator representing the interaction potential between electrons,

$$V^{(\text{ee})}(z) = zV_{\text{phys}}^{(\text{ee})} + (1-z)V_{\text{HF}}^{(\text{ee})}, \quad (4)$$

where

$$V_{\text{phys}}^{(\text{ee})} = \sum_{i<j} r_{ij}^{-1} \quad (5)$$

in atomic units, and $V_{\text{HF}}^{(\text{ee})}$ represents the Hartree-Fock mean-field interaction,

$$V_{\text{HF}}^{(\text{ee})} = \sum_{j,k} [J_k(\mathbf{x}_j) - K_k(\mathbf{x}_j)]. \quad (6)$$

The J_k and K_k are the customary Coulomb and exchange operators, respectively.¹⁴ The summation index k extends over the occupied spin orbitals χ_k , while the index j extends over the electron variables $\mathbf{x}_j=(\mathbf{r}_j, \omega_j)$, where the \mathbf{r}_j are the spatial coordinates and the ω_j are the formal spin variables. The actions of the J_k and K_k on an arbitrary one-particle function $g(\mathbf{x}_j)$ are given by

$$J_k(\mathbf{x}_j)g(\mathbf{x}_j) = g(\mathbf{x}_j) \int \frac{|\chi_k(\mathbf{x})|^2}{|\mathbf{r}_j - \mathbf{r}|} d\mathbf{r} d\omega \quad (7)$$

and

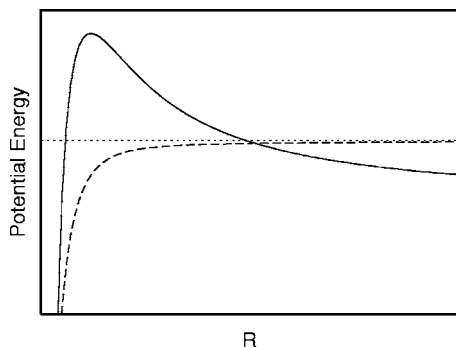


FIG. 1. Schematic representation of the total potential-energy function for the migration of a rigid electron cluster to a distance R off the nuclear framework. The solid curve corresponds to a sufficiently negative value of the perturbation parameter z . The dashed curve corresponds to $z=0$.

$$K_k(\mathbf{x}_j)g(\mathbf{x}_j) = \chi_k(\mathbf{x}_j) \int \frac{\chi_k^*(\mathbf{x})g(\mathbf{x})}{|\mathbf{r}_j - \mathbf{r}|} d\mathbf{r}d\omega. \quad (8)$$

Note that the J_k and K_k are independent of z . The χ_k are the usual Hartree-Fock spin orbitals, obtained from the Hamiltonian at $z=0$.

Consider a hypothetical situation in which all N electrons move as a rigid cluster with fixed positions relative to each other but with freedom to collectively migrate off the nuclear framework. The behavior of the potential-energy operator $V(z)$ as a function of the distance of this cluster from any given nucleus provides a simple heuristic illustration of the proposed critical phenomenon. Let R be the distance between some given electron in the cluster and some given nucleus in the fixed nuclear framework. In the limit of small R the attractive Coulomb potential $V^{(ne)}$ predominates over the other terms in $V(z)$. At large R it is the term $zV_{\text{phys}}^{(ee)}$ that predominates. The spatial parts of the χ_k fall off exponentially with distance from the nuclei.¹⁵ Thus, if electron j is a large distance from the nuclear framework, the operator $J_k(\mathbf{x}_j)$ approaches the simple repulsive Coulomb potential $1/R$, while the effect of the exchange operator decays to zero much more rapidly. With all electrons far away from the nuclear region,

$$V(z) \approx \left[-(N-1)z + N - Z_{\text{tot}} - 1 \right] \frac{N}{R} + z \sum_{i < j} r_{ij}^{-1}, \quad (9)$$

where Z_{tot} is the sum of the charges of all the nuclei. The first term on the right-hand side is repulsive when $z < 1 - Z_{\text{tot}}/(N-1)$ and increases with decreasing R . Interpolating between this small- R and large- R behavior, we obtain a schematic representation of the potential given by the solid curve in Fig. 1.

In the limit of infinite R , the r_{ij} remain finite and the electronic Hamiltonian becomes simply

$$H(z) = -\frac{1}{2} \sum_i \nabla_i^2 + z \sum_{i < j} r_{ij}^{-1}. \quad (10)$$

Making a change of variables in Eq. (10) to $\mathbf{q}_i = -z\mathbf{r}_i$, it is easy to show that the z dependence of the quantized energy levels of the electron cluster is simply

$$E_c^{(N)}(z) = z^2 \epsilon^{(N)}, \quad (11)$$

where the discrete levels $\epsilon^{(N)} < 0$ are those which occur for the special case $z=-1$. The effect of a sufficiently negative value of z is to create a barrier at intermediate distance and to narrow the well at the nucleus. As z becomes more negative, the barrier for the electrons to escape increases, and the well in the nuclear region also narrows. At some critical value z_c the ground state of the bound manifold in the nuclear well becomes equal to $E_c^{(N)}$ and the electrons can depart from the nuclear framework by tunneling through the barrier. For $z < z_c$, the Hamiltonian exhibits a continuum of eigenstates in which the electrons are dissociated from the nuclear framework and exist in a collective scattering state relative to the fixed nuclear configuration (within the Born-Oppenheimer approximation).

Thus, the conclusion that a singular point exists at negative z follows from the fact that at large negative z the repulsive interelectron interactions are spatially limited to the region of the nuclei while the interelectron attraction is not. This analysis is a special case of a more general analysis of many-body perturbation theories presented earlier by Baker in the context of nuclear physics.¹⁶ Baker suggested that z_c is analogous to a critical point in an (E, z) phase diagram. For real z beyond z_c the Hamiltonian will not support a bound state of all the particles. This is similar to the situation in which the nuclear charge Z of an atom is treated as a continuous parameter. The energy can be obtained as an asymptotic series in $1/Z$. For any atom there exists a critical charge below which the atom will spontaneously ionize,¹⁷⁻²¹ resulting in a singular point at some positive value of $1/Z$. Similar behavior is also seen in the semiclassical $1/D$ expansion of atomic and molecular energies, where D is the spatial dimensionality.²²⁻²⁹ Another analog is the general phenomenon of spatial and/or spin symmetry breaking in Hartree-Fock electronic reference wave functions, a topic with an extensive literature.³⁰⁻³⁹ Perhaps the best-known example is the restricted to unrestricted Hartree-Fock (RHF to UHF) orbital instability that develops at intermediate bond distances during the homolytic cleavage of chemical bonds.⁴⁰ Mathematical conditions for the existence of critical points for orbital instabilities have been known for some time.³²⁻³⁵

In statistical mechanics critical points correspond to singular points,⁴¹ typically of algebraic form. In the case of the perturbation theories for the Schrödinger equation, the dissociation at the critical point comes about by tunneling through a potential-energy barrier, which results in a more complicated functional form. An analysis of the $1/Z$ series for the two-electron atom²⁰ has suggested that the singularity can be described by a confluent hypergeometric function.

It is also of interest to consider the behavior of the MP energy function for positive values of z beyond the physical point $z=1$. The interelectron potential is repulsive and its magnitude is increased by a factor of z , while the mean-field potential, multiplied by $(1-z)$, becomes attractive for $z > 1$. It is not obvious in advance which of these two effects will predominate in the region of the nuclear framework. If it is the repulsion, then there could come a value of z at which the energy could be lowered by ejecting an electron. This would

be a critical point on the positive real z axis corresponding to one-electron ionization. Indeed, there might be a series of one-electron ionizations as z becomes increasingly positive.

III. ANALYSIS OF CONFIGURATION-INTERACTION EIGENVALUES

In practice, MP perturbation series are computed within the approximation of a finite one-particle basis set;⁹ i.e., the Hartree-Fock molecular orbitals used to construct the many-body wave functions are represented in terms of a finite set of atomic, typically Gaussian, functions. The exact many-body solution for the finite one-particle basis is the full-configuration-interaction (FCI) wave function, a variationally optimized linear combination of all Slater determinants resulting from the distribution of the electrons in the molecular orbitals in all possible ways. The MP perturbation series is the asymptotic expansion of the FCI eigenvalue function, $E_{\text{FCI}}(z)$.⁹ This function can be obtained by constructing the z -dependent Hamiltonian matrix using Eq. (1) and then determining the eigenvalues of the matrix by numerical diagonalization for given z values.

The singularity structure of these eigenvalue functions in the complex z plane can be derived from first principles. One can prove^{20,42} that the singular points occur in complex-conjugate pairs with nonzero imaginary parts, and in the neighborhood of each singular point the function behaves as a square-root branch point. This would seem to contradict the Stillinger conjecture, which requires a critical point on the real axis. In fact, there is no contradiction because Stillinger's analysis applies to the true $E(z)$, not to $E_{\text{FCI}}(z)$ within a finite atom-centered basis. Another difference between these two functions is that the FCI spectrum consists only of discrete bound states while the true spectrum contains an ionization continuum. At z_c the ground state is expected to pass into the continuum. $E(z)$ becomes complex beyond z_c while $E_{\text{FCI}}(z)$ remains real.

What then is the significance of the MP critical point of $E(z)$ for the corresponding $E_{\text{FCI}}(z)$? One might expect that $E_{\text{FCI}}(z)$ would try to model a continuum at z_c with a grouping of discrete but closely spaced eigenstates that undergo sharp avoided crossings with the ground state.¹⁷ To answer this question, we have computed configuration-interaction energy eigenvalues of the z -dependent Hamiltonian for various systems. The computational method and the basis sets are described in detail in Appendix A.

The FCI spectrum for the He atom as a function of z , using the augmented correlation-consistent polarized valence quadruple-zeta (aug-cc-pVQZ) basis set, is shown in Fig. 2. This basis belongs to the family of correlation-consistent polarized valence X -tuple zeta (cc-pVXZ) Gaussian sets augmented with diffuse functions.⁴³⁻⁴⁵ These sets are widely used for high-accuracy *ab initio* quantum chemistry. What we have plotted in Fig. 2 and in all of the subsequent $E(z)$ diagrams is actually the quantity

$$\epsilon^{(j)}(z) = E^{(j)}(z) - (E_0 + E_1 z), \quad (12)$$

where the $E^{(j)}(z)$ are the eigenvalues, with j labeling different eigenstates. The MP series coefficients E_0 and E_1 corre-

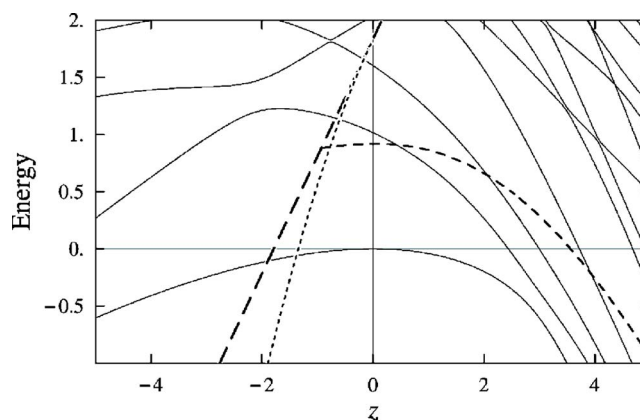


FIG. 2. Energies $\epsilon^{(j)}(z) = E^{(j)}(z) - (E_0 + E_1 z)$, in units of E_h , of the FCI spectrum for $1S$ states of the He atom as a function of the perturbation parameter z , with the aug-cc-pVQZ basis. The full ionization limit $E(z)=0$ corresponds to the large-dash line while the limit of one-electron ionization is shown by the small-dash curve. The limit for dissociation into a bound dielectron corresponds to the dotted curve.

spond to the ground state. E_1 is much larger than subsequent E_i and its value for low-lying excited states is not too different from the value for the ground state. Therefore, $\epsilon^{(j)}$ for low-lying states is approximately parallel to the z axis, and this more clearly displays the relative spacing of the energy levels than would a plot of $E^{(j)}$. $\epsilon^{(0)}$ is zero at $z=0$, and at the physical point $z=1$ it is equal to the correlation energy. Thus, $\epsilon^{(0)}(z)$ can be thought of as a z -dependent generalization of the ground-state correlation energy. For $j>0$, however, $\epsilon^{(j)}(z)$ is the difference between the energy of an excited state and the Hartree-Fock energy of the ground state.

The dotted curve in Fig. 2 corresponds to the energy of a bound dielectron. Separating out the motion of the center of mass in Eq. (10) makes this an exactly solvable two-body problem, with ground-state energy $-z^2/4$. The large-dash line shows the total dissociation limit, given by setting $E^{(j)}(z) = 0$ in Eq. (12). The small-dash curve shows the limit for one-electron ionization obtained using a direct numerically exact computation, as described in Appendix A. Bound eigenstates of $H(z)$ can exist only in the (E, z) region between the dotted and small-dash curves.

There is no evidence from the FCI spectrum in Fig. 2 of a dissociation continuum at negative z . Along the *positive* real z axis there is a broad avoided crossing at $z=3.0$, but this represents an interaction between the ground state and the $1s2s\ 1S$ excited state. It corresponds to a complex-conjugate pair of square-root branch points in $E(z)$, with real parts of the singular points equal to the point of closest approach of the two interacting curves for a path along the real axis. (See Appendix B.) There is also a very broad isolated avoided crossing at $z \approx -13$, the position of which, in contrast to the position of the avoided crossing at positive z , depends strongly on the choice of basis set. Increasing the basis size to augmented correlation-consistent polarized valence sextuple zeta (aug-cc-pV6Z) moves the avoided crossing to $z = -5.7$, while decreasing the size to aug-cc-pVDZ causes it to disappear. But even with the larger basis, the crossing at negative z represents an isolated interaction between the ground state and a single bound excited state.

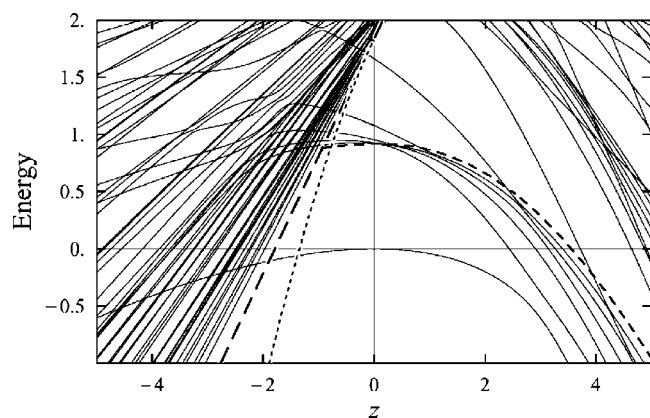


FIG. 3. Energies $\epsilon^{(j)}$, in E_h , of the FCI spectrum for $1S$ states of the He atom as a function of the perturbation parameter z , with the diffuse even-tempered aug-cc-pVQZ-*et3* basis. As in Fig. 2, the large-dash line, the small-dash curve, and the dotted curve show the full ionization, one-electron ionization, and bound dielectron limits, respectively.

Figure 3 shows results from an extremely diffuse basis (“aug-cc-pVQZ-*et3*”) constructed by adding to the aug-cc-pVQZ basis additional Gaussian functions with exponents chosen according to an even-tempered scheme, as described in Appendix A. The structure of the FCI spectrum at positive z is similar to that in the previous examples, but now the structure at negative z is quite different. A group of very sharp crossings is evident, beginning at $z=-2.2$. In fact, the crossings are avoided but they approach so closely that this cannot be discerned within the resolution of the plot. The z value at the onset of the sharp crossings can be decreased by adding even more diffuse functions, but the limit, obtained by setting the Gaussian exponents almost to zero, is the full ionization limit, not the limit of the bound dielectron.

One-electron functions centered at the nucleus are not well suited for describing a dielectron cluster dissociated from the nucleus. A simple way to construct a basis set valid over a wide range of both positive and negative z is to augment the basis with a “ghost” atom far away from the

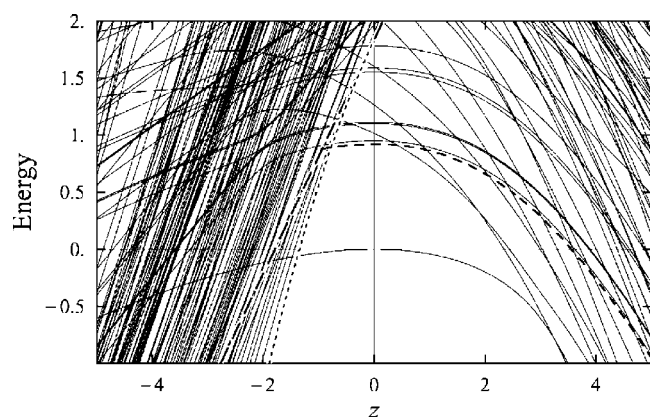


FIG. 4. Energies $\epsilon^{(j)}$, in E_h , of the FCI spectrum of He for those states for which the overlap with the $1S$ ground-state wave function is nonvanishing within the precision of the computation, as a function of the perturbation parameter z , with an aug-cc-pVQZ basis centered at the nucleus further augmented with a ghost hydrogen aug-cc-pVQZ basis centered 1000 Å away. As in Fig. 2, the large-dash line, the small-dash curve, and the dotted curve show the full ionization, one-electron ionization, and bound dielectron limits, respectively.

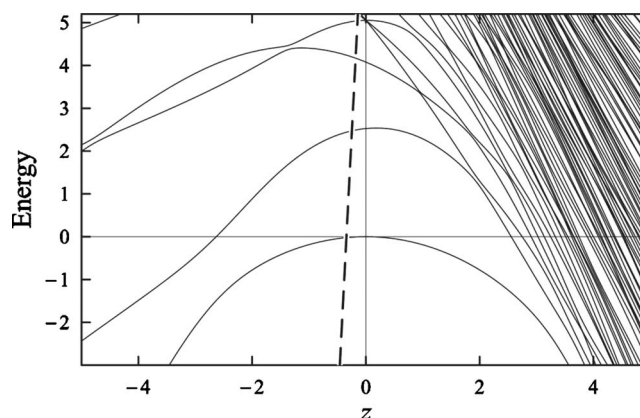


FIG. 5. Energies $\epsilon^{(j)}$, in E_h , of the CI spectrum for $1S$ states of the Ne atom as a function of the perturbation parameter z , with the cc-pVDZ basis. The dashed curve shows the limit of ionization to free valence electrons.

nucleus. The ghost atom consists merely of basis functions centered at this position but with no nuclear charge. Basis functions centered at the nucleus describe the system for positive z and for negative z before the critical point, and the ghost functions can describe a dielectron that has left the nucleus. Results are shown in Fig. 4. Specifically, we used an aug-cc-pVQZ basis centered at the He nucleus and an aug-cc-pVQZ basis for a ghost hydrogen atom 1000 Å away. The discrete spectrum of the dielectron can now be seen, starting just beyond the dielectron value of z_c .

Figures 5 and 6 show CI results for the Ne atom with the cc-pVDZ and aug-cc-pVDZ basis sets, respectively. These sets differ in that the latter is supplemented with diffuse s , p , and d functions.⁴⁵ These are frozen-core computations; determinants with excitations of the $1s$ electrons are omitted from the CI wave function. As a consequence, the electron cluster we expect to form after z passes through the critical point will consist only of the eight valence electrons. The dashed curves in the figures correspond to dissociation into eight free electrons and an Ne^{8+} ion with a frozen $1s$ core. Because of the large sizes of the basis sets, we have truncated the Hamiltonian matrices by configuration selection. (See Appendix A for details.)

Without the diffuse functions, the level structure at nega-

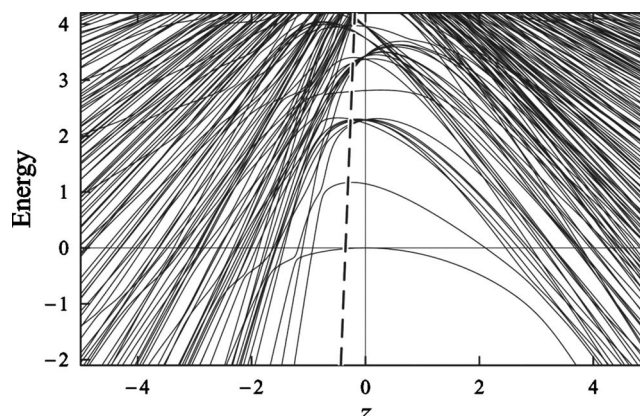


FIG. 6. Energies $\epsilon^{(j)}$, in E_h , of the CI spectrum for $1S$ states of the Ne atom as a function of the perturbation parameter z , with the aug-cc-pVDZ basis. The dashed curve shows the limit of ionization to free valence electrons.

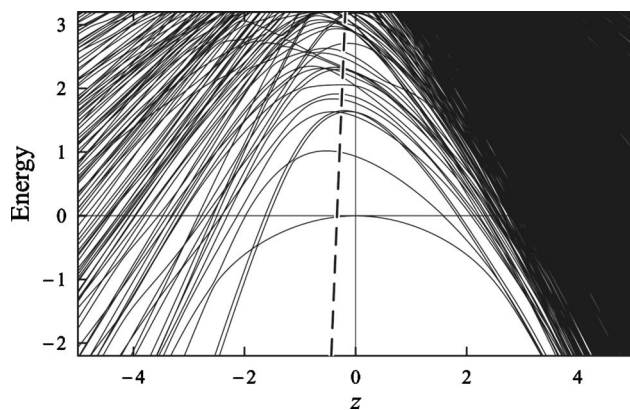


FIG. 7. Energies $\epsilon^{(j)}$, in E_h , of the CI spectrum for $1\Sigma^+$ states of the hydrogen fluoride molecule as a function of the perturbation parameter z , with the cc-pVDZ basis and internuclear separation of 0.916 94 Å. The dashed curve shows the limit of ionization to free valence electrons.

tive z for Ne (Fig. 5) is quite simple, showing a broad isolated avoided crossing with the ground state at $z=-2.4$. The level structure is very different with the aug-cc-pVDZ basis (Fig. 6). In that case the basis is sufficiently diffuse to model a continuum. Many new curves are now present that have very sharp avoided crossings with the diabatic continuation of the ground-state energy at negative z values. The first of these new crossings is at $z=-0.9$, which is somewhat beyond the critical point for full ionization of the eight valence electrons. Adding very diffuse functions brings the continuum down to the full ionization limit. By augmenting the basis on the Ne nucleus with another basis for a ghost F atom far from the Ne nucleus, the initial crossing can be moved to before the full ionization limit.

The hydrogen fluoride molecule is isoelectronic to Ne and with the aug-cc-pVDZ basis its level structure as a function of z is similar to that for Ne. However, with the nonaugmented cc-pVDZ basis, as shown in Fig. 7, the results are qualitatively different from the corresponding Ne results. In contrast to the Ne case, hydrogen fluoride, even with this compact basis, has excited states that cross through the ground state at negative z , although the density of the states is less than that for the critical points in the previous examples with the augmented bases. The reason is that the basis functions centered on the H atom are able to model a cluster of the valence electrons in the same way that the ghost-atom basis functions did this for the He and Ne atoms. The repulsive mean-field potential is much stronger in the neighborhood of the F nucleus than in the neighborhood of the H nucleus, and it becomes more important, in proportion to the factor $(1-z)$, as z becomes more negative. At some point on the negative z axis, this effect will become strong enough to make the valence electrons jump to the hydrogen side of the molecule, causing a critical point to appear. The resulting singularity structure is not too much closer to the origin of the z plane than is the singularity for the isolated avoided crossing in cc-pVDZ Ne. Although the singularity structures of these two systems are quite different, the effect on the convergence of the partial sums of the energy series⁴ is similar.

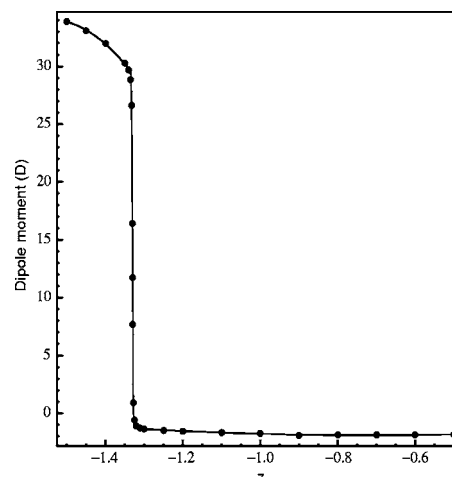


FIG. 8. Ground-state dipole moment of the hydrogen fluoride molecule as a function of the perturbation parameter z , as computed from the FCI wave function using the cc-pVDZ basis.

To test this explanation we carried out FCI computations as a function of z for the hydrogen fluoride molecule and then used the ground-state wave function to compute the value of the dipole moment. The computations were performed using a modified version of the DETCI module of the PSI3 software package^{5,46} Beyond the critical point, we expect to have, in effect, a H^{7-} ion separated from a F^{7+} ion by the physical hydrogen fluoride ($z=1$) bond distance of 0.916 94 Å. This would imply that the dipole moment vector would have a length of 30.83 D, pointing toward the hydrogen. Figure 8 shows the FCI results. Before the critical point, the value of the dipole moment is quite stable with a magnitude of approximately 2 D. At $z=-1.3$ it undergoes a sudden change of sign and stabilizes at approximately 35 D, which is consistent with our explanation.

Figure 9 shows the spectrum for the Ar atom with the cc-pVDZ basis. The level structures at negative z are similar to those for Ne with the corresponding basis. However, at positive z the first excited-state eigenvalue now approaches very close to the ground-state energy, in contrast to the broad avoided crossing in the case of Ne. Figure 10 shows the

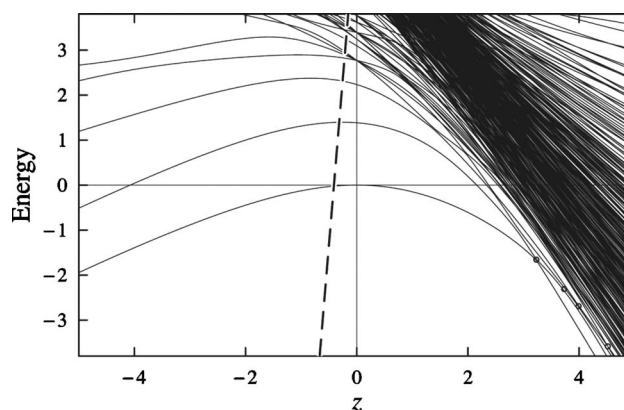


FIG. 9. Energies $\epsilon^{(j)}$, in E_h , of the CI spectrum for $1S$ states of the Ar atom as a function of the perturbation parameter z , with the cc-pVDZ basis. The dashed curve shows the limit of ionization to free valence electrons. Circles mark the points of closest approach of excited states with the diabatic continuation of the ground state at positive z .

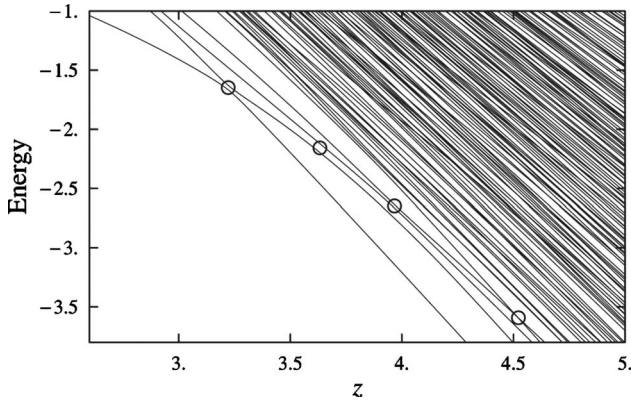


FIG. 10. Expanded view of energies $e^{(j)}$, in E_h , of the CI spectrum for 15 states of the Ar atom as a function of the perturbation parameter z , with the cc-pVDZ basis. Circles mark the points of closest approach of excited states with the diabatic continuation of the ground state at positive z .

approach in more detail. The diabatic continuation of the Ar ground state can be seen to undergo a series of close avoided crossings.

The valence electrons in Ar are farther from the nucleus than in Ne. As z increases beyond $z=1$ the mean-field central potential, although attractive, is less able to counter the increased interelectron repulsion than in the case of Ne. The close crossings in the figure might represent a critical point for ionization to a free electron and an Ar^+ ion. Alternatively, they could represent crossings with a series of Rydberg states, with one electron far from the nucleus. Indeed, our exact analysis of the He case reveals that a single-ionization envelope (shown in Figs. 2–4) should be expected for positive z , and Rydberg states should be encountered prior to reaching this continuum. The closeness of the approach of the curves would be due to the fact that there is very little overlap between the eigenfunctions for the Rydberg state and the ground state.

IV. ANALYSIS OF SUMMATION APPROXIMANTS

The positions of singular points of $E_{\text{FCI}}(z)$ in the complex z plane can be estimated by fitting quadratic summation approximants to the MP series.^{10,47} These approximants are functions of the form

$$S_{[L/M,N]}(z) = \frac{1}{2Q_M} (P_L \pm \sqrt{P_L^2 - 4Q_MR_N}), \quad (13)$$

where P_L , Q_M , and R_N are polynomials in z of degrees L , M , and N , respectively. Note that $S_{[L/M,N]}(z)$ will have a square-root branch point at each nondouble root of the discriminant polynomial

$$D_{[L/M,N]} = P_L^2 - 4Q_MR_N. \quad (14)$$

Because the series coefficients E_i are real numbers, these roots will either lie on the real axis or will exist as complex-conjugate pairs. For this reason, a quadratic approximant would seem to have an appropriate functional form for modeling $E_{\text{FCI}}(z)$, thus providing an alternative to the CI plots for obtaining information about the singularity structure.

TABLE I. Branch-point locations of FCI energy function from analysis of quadratic approximant with index $[L/M,N]$ of MP series and from fitting directly to explicit FCI energy values.

System (basis)	$[L/M,N]$	Branch pts. from series approximants	Branch pts. from fit to FCI energies
Ne (cc-pVDZ)	[6/5,6]	$-2.62 \pm 0.90i$	$-2.63 \pm 0.90i$
	[5/5,6]	$3.14 \pm 0.5i$	$3.12 \pm 0.61i$
HF (cc-pVDZ)	[7/6,7]	-1.30	-1.33
	[6/6,7]	$-1.30 \pm 0.04i$	
Ar (cc-pVDZ)	[6/6,7]	$2.51 \pm 0.37i$	$2.44 \pm 0.46i$
		2.8	
Ar (cc-pVDZ)	[4/4,4]	3.3	$2.8 \pm 0.02i$
		3.7	
Ne (aug-cc-pVDZ)	[4/4,5]	$1.2 \pm 4.0i$	
	[11/11,11]	$-0.824 \pm 0.007i$	
HF (aug-cc-pVDZ)		-0.892	
	[6/6,7]	$3.0 \pm 0.6i$	
HF (aug-cc-pVDZ)	[8/8,8]	$-0.759 \pm 0.015i$	
		-0.771	
Ar (aug-cc-pVDZ)	[7/7,8]	$1.94 \pm 1.0i$	
		$2.03 \pm 1.0i$	
Ar (aug-cc-pVDZ)	[6/6,6]	$-1.24 \pm 0.01i$	-1.183
		-1.5	
	[6/6,7]	2.58	$2.43 \pm 0.08i$

We use the normalization condition $Q_M(0)=1$. The rest of the polynomial coefficients are determined by setting the Taylor series of $S_{[L/M,N]}(z)$ equal to the MP series, according to the asymptotic equation

$$Q_ME^2 - P_LE + R_N \sim \mathcal{O}(z^{L+M+N+2}), \quad (15)$$

which means that the coefficients of the power series in z of the left-hand side are equal to zero through order $z^{L+M+N+1}$. E in Eq. (15) represents the power series for the energy. Collecting terms according to the power of z yields a set of $L+M+N+2$ simultaneous linear equations that determines the polynomial coefficients. It is convenient to express the power series in the form

$$E = (E_0 + E_1) + E_2z + E_3z^2 + E_4z^3 + \dots \quad (16)$$

because $E_0 + E_1$ is the Hartree-Fock energy and E_0 and E_1 are usually not separately reported. This amounts to analyzing a function

$$\tilde{E}_{\text{FCI}}(z) = E_0 + \frac{1}{z}[E_{\text{FCI}}(z) - E_0], \quad (17)$$

which has the same branch point structure as E_{FCI} .

Because the MP series is an asymptotic expansion about the origin of the complex z plane, branch points closer to the origin will be modeled more accurately than those farther away. The number of branch points with converged results for their locations will increase as the order of the series is increased, although at very high order we find that roundoff error in the series coefficients causes spurious branch points to appear. The singularity positions from quadratic approximants are listed in the third column of Table I. The perturbation series were computed to high order with high precision with the PS13 software package.^{5,46,48} Results are shown

for the highest order feasible, as determined by adding a random error to the last digit of the E_i and noting the effect on the computed branch-point positions. We show only the branch points that seem to converge.

The roundoff error enters at a lower order for the series with compact basis sets than for those with augmented basis sets, because the three examples with a compact basis have no singularity within the disk of unit radius in the complex plane. Therefore, the partial sums of the energy series are convergent at $z=1$, which implies that the series coefficients become smaller as the order increases. Eventually, the series coefficients become equal to zero within the finite precision of the computation and yield no further information for fitting the approximants. There is no such problem for the systems with augmented basis sets because their partial sums are divergent at $z=1$.

The magnitude of the imaginary part of the branch-point location is related to the sharpness of the avoided crossing. For an isolated avoided crossing, one can model the interaction between the two states using a two-dimensional matrix eigenvalue equation.⁴⁹ The two eigenvalues are connected by a complex-conjugate pair of square-root branch points. We show in Appendix B that the closest approach along the real z axis occurs when z is equal to the real part of the branch-point pair, and the separation at closest approach between the two states is, to a good approximation,

$$\Delta E_{\min} = |(\sigma_- - \sigma_+) \text{Im } z_s|, \quad (18)$$

where z_s and z_s^* are the singularity locations and σ_- and σ_+ are the diabatic slopes for the two states. A very small value of ΔE_{\min} implies that the crossing is almost diabatic, with very little interaction between the two energy curves, while a large value implies strongly interacting states. The amount of interaction between energy curves should be an indicator of whether or not the singularity structure of $E(z)$ being modeled corresponds to a simple square-root branch point or to a critical point. Small values of ΔE_{\min} should be characteristic of critical points because the eigenfunction of the upper state should have very little spatial overlap with the eigenfunction of the ground state, and hence the connecting matrix elements should be small.

The plots of the spectra in Sec. III are in qualitative agreement with the results in Table I. For example, Ne with the cc-pVDZ basis has a broad avoided crossing near $z=-2.7$ in Fig. 5 and the corresponding imaginary part in Table I is rather large, while the sharp crossings at negative z for aug-cc-pVDZ Ne in Fig. 6 correspond to a group of closely spaced branch points that the quadratic approximant places directly on the real axis. An analysis of the curves in Fig. 5 predicts branch points at $-2.66 \pm 0.98i$ and $3.31 \pm 0.64i$. Quadratic approximant analysis of the MP series gives $-2.62 \pm 0.90i$ and $3.14 \pm 0.5i$. The agreement is not quantitative because the MP series corresponds to the full CI energy while the curves in the figures were generated from truncated CI computations. In principle, $\text{Im } z_s$ can be determined from the curves by estimating σ_- , σ_+ , and ΔE_{\min} and using Eq. (18). However, because that equation comes from a 2×2 matrix approximation the accuracy can be adversely affected

by the presence of other nearby crossings. We find that a 3×3 matrix approximation is more satisfactory and have employed it in the analysis of the figures.

To more rigorously determine branch-point locations and thereby assess the accuracy of the z_c predictions from quadratic approximants and from truncated CI computations, we adapted the PSI3 code^{5,46} to explicitly compute FCI eigenvalues of $H(z)$ along the real axis. Exact $E(z)$ values (within the chosen finite basis set) for the subspace of lowest-lying electronic states were determined iteratively using a modified block Davidson algorithm.⁵⁰ This approach is more costly than the indirect analysis of $E_{\text{FCI}}(z)$ based on the MP series because it uses, in effect, a separate FCI computation at each value of z , but it provides an independent check of the quadratic approximant analysis without the error of the truncated CI computations. To extract a singularity position from the $E(z)$ values, we fit a 3×3 matrix eigenvalue function to several ground-state $E(z)$ points surrounding an avoided crossing.

The iterative subspace procedure for the FCI computations worked well in uncongested areas, but in regions of z where the spectrum was crowded with numerous sharp avoided crossings, convergence difficulties were often encountered. (The truncated CI approach used to generate the figures of Sec. III did not suffer from such problems because the complete eigenspectrum of the truncated matrix was computed by standard, noniterative methods that do not resort to subspace expansions.) Our FCI branch points, for cases in which we obtained convergence, are listed in Table I alongside the results from the MP series analysis. The excellent agreement between the corresponding z_c values nicely demonstrates the ability of quadratic approximants of high-order MP series to accurately locate FCI branch points.

V. DISCUSSION

The singularity structure in the negative half plane of the perturbation parameter z for the MP energy function $E(z)$ depends strongly on the choice of basis set. Stillinger's conjecture¹³ that there will be a critical point at some negative real value of z corresponding to dissociation into a bound electron cluster free from the nuclei is based on an analysis of the Hamiltonian without a finite basis set approximation. In practice, MP computations are performed with a finite basis, which means that the relevant function is the FCI energy $E_{\text{FCI}}(z)$. Depending on the basis set, $E_{\text{FCI}}(z)$ may or may not have a singularity structure resembling that of $E(z)$. In particular, a basis set constructed from functions centered on the nuclei cannot efficiently model a situation in which the electrons are bound together as a pseudoparticle that is not bound to the nuclei. We find that for computations using standard basis sets augmented with diffuse functions, E_{FCI} can have a group of branch points very close to the real axis that correspond to a critical point in $E(z)$, but the physical process occurring at that point is complete dissociation rather than formation of an electron cluster.

Our analysis resolves the apparent disagreement between Stillinger's suggestion that class B series behavior is caused by a critical point and the conclusion of a study by Olsen *et*

*al.*⁴⁹ that it is caused by an avoided crossing with an excited state. Olsen *et al.* used a 2×2 matrix eigenvalue equation as an approximant for $E_{\text{FCI}}(z)$ and found that the dominant singularity structure for class B systems consisted of a complex-conjugate pair of square-root branch points. By construction, this approximant has only one such pair. It can model only one branch-point pair at a time of the grouping of branch points that $E_{\text{FCI}}(z)$ uses to model a critical point. Olsen *et al.* studied the first pair in the grouping and noted that with augmented basis sets its location approached the continuum energy for complete dissociation, which is consistent with our findings from CI plots and quadratic-approximant series analyses. In other words, the “backdoor intruder” state, which can spoil the convergence of the MP series, is the completely ionized state represented in a limited diffuse atom-centered basis set.

In general, we predict that atoms will have the critical-point singularity structure in the negative half plane only if a sufficiently diffuse basis set is used. Molecules, however, may show this singularity structure even with compact basis sets, due to a migration of the electrons within the molecule. Basis functions on less electronegative atoms can model a cluster of valence electrons that have moved away from the more electronegative atoms due to the increasing magnitude of the mean-field repulsion. This effect should be most important, occurring at relatively smaller $|z|$ values, when highly electronegative atoms are present. A new result from the present work is the observation that $E_{\text{FCI}}(z)$ for the Ar atom has singularity structure in the positive half plane very close to the real axis, indicating either a critical point for one-electron ionization or a sharp avoided crossing with a Rydberg state. In contrast, for Ne the first singularity in the positive half plane corresponds to a broad avoided crossing with another bound state.

The primary motivations for studying the singularity structure of the MP energy function are to develop methods for predicting the accuracy of MP4 computations and for improving that accuracy by modeling the dominant singularity.^{10,39,51,52} Critical points can exist within the unit circle, and in such cases the MP series will be divergent. Although MP2 may still be dependable, adding higher-order terms of a divergent series will, at some high enough order, begin to decrease the accuracy. It is now clear that MP4 series should not in general be summed by simply adding together the terms in the perturbation series; much more dependable results can be obtained from the MP4- $q\lambda$ summation approximant.⁵³ The $q\lambda$ approximant uses a repartitioning of the Hamiltonian to shift the singularity positions so as to optimize the series summation by a quadratic approximant. (The use of a quadratic approximant ensures that the summation will converge even if the series itself diverges.⁴⁷) The locations of the singularities for the purpose of this optimization are determined from the roots of the discriminant polynomial $D_{[L/M,N]}$ of Eq. (14). Fourth order is, in general, quite low for an asymptotic series analysis. In the high-order limit the series coefficients are determined by the asymptotic series of the dominant singularity, according to Darboux’s theorem,^{12,54} but at fourth order one can expect nonsingular effects and effects of nondominant singularities to still be

significant. The effective use of the $q\lambda$ method depends on having some idea of how accurately the singularities of the fourth-order approximant model the true singularity structure.

A low-order quadratic approximant works best when the dominant singularity of the underlying function is an isolated square-root branch-point pair. In such cases, for example, the molecules BH, CH₂, NH₂, CH₃, and H₂O⁺, the $q\lambda$ approximant can reduce the summation error by an order of magnitude.^{51,53} For systems in which the dominant singularity of the underlying function is a critical point, the improvement from the approximant is more modest. In applying the $q\lambda$ approximant, one must choose whether to model the singularity structure in the positive or the negative half plane. This choice can be made on the basis of the approximant’s own estimates of the various singularity positions. However, the branch points in $E_{\text{FCI}}(z)$ that describe a critical point have very small imaginary parts, orders of magnitude smaller than the imaginary parts of the “true” square-root branch points that correspond to avoided crossings in both $E(z)$ and $E_{\text{FCI}}(z)$. A branch-point pair with small imaginary part behaves at a distance as a double root of $D_{[L/M,N]}$. Because $D_{[L/M,N]}^{1/2}$ is nonsingular at a double root, such branch points will be harder to detect than branch points with larger imaginary parts, and in an analysis using a series of only fourth order they seem to be farther from the origin than they actually are.

The position of the critical points of the exact $E(z)$ can easily be estimated even with very-low-order perturbation theory. For example, for He the critical point for complete ionization can be estimated from MP2 simply by setting the partial sum equal to zero, according to

$$z_c = \frac{1}{2E_2} \left(-E_1 \pm \sqrt{E_1^2 - 4E_0E_2} \right). \quad (19)$$

Using the aug-cc-pVDZ basis, this gives $z_c = -1.918$, which is in excellent agreement with the exact result, -1.893 . However, the position of a critical point in $E_{\text{FCI}}(z)$, which is the information most relevant for MP series summation, is much harder to calculate. By taking into account the known position of z_c in $E(z)$, the position of the branch point in the MP4- $q\lambda$ approximant, and the qualitative understanding we have presented here of the accuracy with which a given kind of basis set can model the dissociation of the system, it may be possible to develop a procedure for reliably estimating the position of z_c in $E_{\text{FCI}}(z)$ using fourth-order series.

In principle, the singularity structure could be taken as a consideration in choosing a basis set. Removing diffuse functions from the basis will eliminate the critical point at negative z or at least shift it away from the origin, lessening its significance. Unfortunately, as has been pointed out previously,^{3,4,49} the systems for which the negative- z critical-point singularity is dominant are very often the same systems for which diffuse functions are needed for an accurate description of the wave function.⁴⁵ Perhaps a more promising strategy is to change the position of the critical point by modifying the partitioning of the Hamiltonian. One method is to change the positions of energy-level crossings by incor-

porating level shifting operators^{55–58} into H_0 . This allows one to arbitrarily specify the unperturbed energy spectrum. Alternatively, the critical-point position can be shifted to an arbitrary position by the Feenberg repartitioning,^{6–8,53,59–61} which effects a conformal mapping of the z plane.⁶² These approaches must be implemented with care because they shift the positions of all singularities, possibly increasing the importance of some other singularity that previously was nondominant.

ACKNOWLEDGMENT

The Chemical Physics Division, Office of Basic Energy Sciences of the U.S. Department of Energy, Grant No. DE-FG02-01ER15226, supported the research performed at the University of Georgia.

APPENDIX A: COMPUTATIONAL DETAILS

Energy computations

Here we describe the procedures that were used to generate $E(z)$ for Figs. 2–7, 9, and 10. CI matrices of $H(z)$ in a many-electron basis of Slater determinants were explicitly constructed from one- and two-electron integrals computed using the MOLPRO2000 software package.⁶³ For all z , the $H(z)$ matrix was properly constructed from the ground-state Hartree-Fock orbitals of the physical Hamiltonian H_0+H_1 . A unitary transformation of the original Hamiltonian matrix was performed to represent $H(z)$ in a basis of configuration state functions with the same spin and angular momentum as the ground electronic state. For He (Figs. 2–4) the full CI matrix was used. For the other systems the CI matrix was truncated in order to allow explicit construction and storage of the CI matrix in core memory. For the initial Hamiltonian matrix, determinants were included in the basis if the corresponding E_0 was below a cutoff value. To determine the cutoff, determinants with the same value of E_0 were grouped into manifolds and then whole manifolds were added to the basis in order of increasing E_0 until the basis dimension was as close as possible to 4000. The subsequent unitary transformation to the configuration state-function representation substantially reduced the basis dimension. All the eigenvalues of the CI matrices were computed, using the eigensystem routine of MATHEMATICA.⁶⁴

To definitively reveal the ionization structure of the exact $E(z)$ spectrum of He for $z > 1$, we used Cooley-Numerov (CN) numerical methods^{65,66} to precisely determine the energy curve for ground-state He^+ . This was implemented using the numerical differential equation solvers in MATHEMATICA.⁶⁴ First, the Hartree-Fock 1s orbital for the He atom was self-consistently converged on a very fine radial grid by a CN algorithm to provide an essentially exact numerical representation of the mean-field potential. The CN procedure was then executed again to compute virtually exact He^+ eigenvalues of $H(z)$. The resulting He^+ energy curve is superimposed on the right side of Figs. 2–4. It provides an infinite-basis exact envelope with which to analyze the finite-basis curves for positive z . Nonetheless, on the coarse scale of the figures, the exact He^+ curve is practically indis-

tinguishable from the curves which would be obtained with the finite QZ basis sets.

Basis sets

Standard correlation-consistent polarized X -tuple zeta (cc-pVXZ) one-particle Gaussian basis sets and their diffuse-augmented analogs (aug-cc-pVXZ) were employed in this study.^{43–45} As the cardinal number X of these atomic orbital sets increases, in the sequence $X=D, T, Q, 5, 6, \dots$, a systematic approach to the complete basis set limit is achieved. Of particular note for our current purposes is the ability of the diffuse aug-cc-pVXZ sets to partially model ionization phenomena. Our extremely diffuse aug-cc-pVQZ-et3 basis set for He was derived from the standard aug-cc-pVQZ $5s4p3d2f$ spherical-harmonic set by a $3s3p3d3f$ even-tempered extension, with diffuse Gaussian function exponents $\zeta_k = c\beta^{k-2}$, $k=1, 2, 3$, where $(c, \beta) = (0.03, 3.804)$, $(0.014, 3.444)$, $(0.029, 3.484)$, and $(0.046, 3.881)$ for the s, p, d , and f manifolds, respectively.

APPENDIX B: AVOIDED CROSSINGS AND BRANCH POINTS

A 2×2 matrix eigenvalue problem provides a simple model for locating complex-valued branch points z_s of $E(z)$ from features of avoided crossings along the real z axis.⁴⁹ Consider the matrix

$$\mathbf{H}_{\text{phys}} = \begin{pmatrix} \alpha & \delta \\ \delta & \beta \end{pmatrix}, \quad (\text{B1})$$

which is partitioned for a perturbation expansion in z in the form $\mathbf{H}(z) = \mathbf{H}_0 + z\mathbf{H}_1$ with

$$\mathbf{H}_0 = \begin{pmatrix} \alpha + \alpha_s & 0 \\ 0 & \beta + \beta_s \end{pmatrix}, \quad \mathbf{H}_1 = \begin{pmatrix} -\alpha_s & \delta \\ \delta & -\beta_s \end{pmatrix}. \quad (\text{B2})$$

The eigenvalues of $\mathbf{H}(z)$ are

$$E_{\pm}(z) = \frac{1}{2}[\alpha + \beta + (1-z)(2\alpha_s + \gamma_s)] \pm \frac{1}{2}\{[\gamma + (1-z)\gamma_s]^2 + 4\delta^2 z^2\}^{1/2}, \quad (\text{B3})$$

where

$$\gamma = \beta - \alpha, \quad \gamma_s = \beta_s - \alpha_s. \quad (\text{B4})$$

The point of closest approach between E_+ and E_- is

$$z_{\min} = \frac{\gamma + \gamma_s}{4\delta^2 + \gamma_s^2}, \quad (\text{B5})$$

at which the difference between the eigenvalues is

$$\Delta E_{\min} = \frac{2|(\gamma + \gamma_s)\delta|}{(4\delta^2 + \gamma_s^2)^{1/2}}. \quad (\text{B6})$$

It follows from Eq. (B3) that the branch points of $E_{\pm}(z)$ are z_s and z_s^* , where

$$z_s = \frac{\gamma + \gamma_s}{4\delta^2 + \gamma_s^2}(\gamma_s + 2\delta i). \quad (\text{B7})$$

Note that $z_{\min} = \text{Re } z_s$.

Let $\phi = \text{Im } z_s / \text{Re } z_s$. Then $\phi = 2\delta / \gamma_s$, and

$$\Delta E_{\min} = |\gamma_s \text{Im } z_s| (1 + \phi^2)^{1/2}. \quad (\text{B8})$$

Let

$$\sigma_{\pm} = \lim_{z \rightarrow \infty} \frac{dE_{\pm}}{dz}. \quad (\text{B9})$$

σ_+ and σ_- are the diabatic slopes of the eigenvalue functions. Taking the derivative of Eq. (B3) with respect to z , one finds that

$$\gamma_s = (\sigma_+ - \sigma_-)(1 + \phi^2)^{-1/2}, \quad (\text{B10})$$

which yields Eq. (18).

The magnitude of the off-diagonal term in the perturbation evaluated at the point of closest approach, $|\delta \text{Re } z_s|$ can be taken as a measure of the amount of interaction between the two eigenstates. If $|\text{Re } z_s|$ is significantly larger than $|\text{Im } z_s|$, which is usually true for the dominant singularities of MP energy functions, then $|\delta \text{Re } z_s| \approx \Delta E_{\min}/2$.

¹ P. J. Knowles, K. Somasundram, N. C. Handy, and K. Hirao, Chem. Phys. Lett. **113**, 87 (1985).

² W. D. Laidig, G. Fitzgerald, and R. J. Bartlett, Chem. Phys. Lett. **113**, 151 (1985).

³ O. Christiansen, J. Olsen, P. Jørgensen, H. Koch, and P.-A. Malmqvist, Chem. Phys. Lett. **261**, 369 (1996).

⁴ J. Olsen, O. Christiansen, H. Koch, and P. Jørgensen, J. Chem. Phys. **105**, 5082 (1996).

⁵ M. Leininger, W. D. Allen, H. F. Schaefer, and C. D. Sherrill, J. Chem. Phys. **112**, 9213 (2000).

⁶ C. Schmidt, M. Warken, and N. C. Handy, Chem. Phys. Lett. **211**, 272 (1993).

⁷ D. Cremer and Z. He, J. Phys. Chem. **100**, 6173 (1996).

⁸ B. Forsberg, Z. He, Y. He, and D. Cremer, Int. J. Quantum Chem. **76**, 306 (2000).

⁹ D. Cremer, in *Encyclopedia of Computational Chemistry*, edited by P. v. R. Schleyer, N. L. Allinger, T. Clark, J. Gasteiger, P. A. Kollman, H. F. Schaefer, and P. R. Schreiner (Wiley, New York, 1998), pp. 1706-1735.

¹⁰ D. Z. Goodson and A. V. Sergeev, Adv. Quantum Chem. **47**, 193 (2004).

¹¹ R. V. Churchill, *Complex Variables and Applications* (McGraw-Hill, New York, 1960).

¹² C. Hunter and B. Guerrieri, SIAM J. Appl. Math. **39**, 248 (1980).

¹³ F. H. Stillinger, J. Chem. Phys. **112**, 9711 (2000).

¹⁴ F. Jensen, *Introduction to Computational Chemistry* (Wiley, New York, 1999), pp. 57-69.

¹⁵ N. C. Handy, M. T. Marron, and H. J. Silverstone, Phys. Rev. **180**, 45 (1969).

¹⁶ G. A. Baker, Jr., Rev. Mod. Phys. **43**, 479 (1971).

¹⁷ F. H. Stillinger, J. Chem. Phys. **45**, 3623 (1966).

¹⁸ E. Brändas and O. Goscinski, Int. J. Quantum Chem., Symp. **6**, 59 (1972).

¹⁹ W. P. Reinhardt, Phys. Rev. A **15**, 802 (1977).

²⁰ J. D. Baker, D. E. Freund, R. N. Hill, and J. D. Morgan III, Phys. Rev. A **41**, 1247 (1990).

²¹ A. V. Sergeev and S. Kais, Int. J. Quantum Chem. **75**, 533 (1999).

²² J. G. Loeser, J. Chem. Phys. **86**, 5635 (1987).

²³ D. D. Frantz and D. R. Herschbach, Chem. Phys. **126**, 59 (1988).

²⁴ D. K. Watson and D. Z. Goodson, Phys. Rev. A **51**, R5 (1995).

²⁵ P. Serra and S. Kais, Phys. Rev. Lett. **77**, 466 (1996).

²⁶ P. Serra and S. Kais, Chem. Phys. Lett. **260**, 302 (1996).

²⁷ P. Serra and S. Kais, Phys. Rev. A **55**, 238 (1997).

²⁸ S.-W. Huang, D. Z. Goodson, M. López-Cabrera, and T. C. Germann, Phys. Rev. A **58**, 250 (1998).

²⁹ Q. Shi, S. Kais, F. Remacle, and R. D. Levine, J. Chem. Phys. **114**, 9697 (2001).

³⁰ E. R. Davidson and S. T. Borden, J. Phys. Chem. **87**, 4783 (1983).

³¹ P.-O. Löwdin, Rev. Mod. Phys. **35**, 496 (1963).

³² J. Čížek and J. Paldus, J. Chem. Phys. **47**, 3976 (1967).

³³ J. Paldus and J. Čížek, Chem. Phys. Lett. **3**, 1 (1969).

³⁴ J. Paldus and J. Čížek, J. Chem. Phys. **52**, 2919 (1970).

³⁵ R. Seeger and J. A. Pople, J. Chem. Phys. **66**, 3045 (1977).

³⁶ W. D. Allen, D. A. Horner, R. L. DeKock, R. B. Remington, and H. F. Schaefer, Chem. Phys. **133**, 11 (1989).

³⁷ J. Olsen, P. Jørgensen, H. Koch, A. Balkova, and R. J. Bartlett, J. Chem. Phys. **105**, 5082 (1996).

³⁸ T. D. Crawford, W. D. Allen, J. F. Stanton, W. D. Allen, and H. F. Schaefer, J. Chem. Phys. **107**, 10626 (1997).

³⁹ D. Z. Goodson and M. Zheng, Chem. Phys. Lett. **365**, 396 (2003).

⁴⁰ A. Szabo and N. S. Ostlund, *Modern Quantum Chemistry: Introduction to Advanced Electronic Structure Theory* (McGraw-Hill, New York, 1989), pp. 221-229.

⁴¹ C. Domb, Adv. Phys. **19**, 339 (1970).

⁴² A. Katz, Nucl. Phys. **29**, 353 (1962).

⁴³ T. H. Dunning, Jr., J. Chem. Phys. **53**, 2823 (1970).

⁴⁴ T. H. Dunning, Jr., J. Chem. Phys. **90**, 1007 (1989).

⁴⁵ R. A. Kendall, T. H. Dunning, Jr., and R. J. Harrison, J. Chem. Phys. **96**, 6796 (1992).

⁴⁶ T. D. Crawford, C. D. Sherrill, E. F. Valeev *et al.*, *PSI 3.2*, 2003. The website for information and downloading the code is www.pscicode.org.

⁴⁷ D. Z. Goodson, J. Chem. Phys. **112**, 4901 (2000).

⁴⁸ In Ref. 5 the tabulated series coefficients were truncated at six decimal digits. Here we used coefficients with the full precision of the computation (with 12 digits beyond the decimal point).

⁴⁹ J. Olsen, P. Jørgensen, T. Helgaker, and O. Christiansen, J. Chem. Phys. **112**, 9736 (2000).

⁵⁰ See the general discussion of CI diagonalization methods in M. L. Leininger, C. D. Sherrill, W. D. Allen, and H. F. Schaefer, J. Comput. Chem. **22**, 1574 (2001).

⁵¹ D. Z. Goodson, J. Chem. Phys. **116**, 6948 (2002).

⁵² D. Z. Goodson, Int. J. Quantum Chem. **92**, 35 (2003).

⁵³ D. Z. Goodson, J. Chem. Phys. **113**, 6461 (2000).

⁵⁴ B. W. Ninham, J. Math. Phys. **4**, 679 (1963).

⁵⁵ D. Hegarty and M. A. Robb, Mol. Phys. **37**, 1455 (1979).

⁵⁶ I. Shavitt and L. T. Redmon, J. Chem. Phys. **73**, 5711 (1980).

⁵⁷ A. Szabados and P. Surjan, Chem. Phys. Lett. **308**, 303 (1999).

⁵⁸ A. Szabados and P. Surjan, J. Chem. Phys. **112**, 4438 (1999).

⁵⁹ E. Feenberg, Phys. Rev. **103**, 1116 (1956).

⁶⁰ Z. He and D. Cremer, Int. J. Quantum Chem. **59**, 71 (1996).

⁶¹ H. H. Homeier, J. Mol. Struct.: THEOCHEM **366**, 161 (1996).

⁶² A. T. Amos, Int. J. Quantum Chem. **6**, 125 (1972).

⁶³ H.-J. Werner, P. J. Knowles, R. Lindh *et al.*, *MOLPRO 2000*, 2000. The website for information and downloading the code is www.molpro.net.

⁶⁴ *MATHEMATICA 5.1*, Wolfram Research, Inc., Champaign, IL, 2003.

⁶⁵ B. Numerov, Publications de l'Observatoire central astrophysique de Russie **2**, 188 (1933).

⁶⁶ J. W. Cooley, Math. Comput. **15**, 363 (1961).